Reflectance confocal microscopy for characterization of mammary ductal structures and development of neoplasia in genetically engineered mouse models of breast cancer

Angela Parrish
Ewa Halama
Maddalena T. Tilli
Matthew Freedman
Priscilla A. Furth
Georgetown University
Lombardi Comprehensive Cancer Center
3970 Reservoir Road NW
Washington, D.C. 20057

Abstract. The earliest steps of breast cancer begin with aberrations in mammary ductal structure. Techniques that enable an investigator to image *in situ* and then analyze the same tissue using biochemical tools facilitates identification of genetic networks and signaling pathways active in the imaged structure. Cellular confocal microscopy (VivaCell-TiBa, Rochester, New York) is used to image mammary ductal structures and surrounding vasculature *in situ* in intact wild-type and genetically engineered mice that develop ERα-initiated ductal carcinoma *in situ* (DCIS) and ERα-driven invasive mammary cancer. In wild-type mice, normal mammary ductal structures that appear from puberty through lactation are visualized and serially sectioned optically, and a developmental atlas is created. Altering tissue preparation enabled visualization of the vasculature surrounding the ductal structures. In the genetically engineered mice, aberrant mammary ductal structures and cancers are imaged and compared to corresponding normal structures. Different preparation techniques are able to preserve tissue for routine histological analyses and RNA isolation. Comparative studies demonstrate that reflectance confocal imaging provides more cellular detail than carmine-alum-stained mammary gland whole mounts and equivalent detail with hematoxylin and eosin stained tissue sections. In summary, reflectance confocal microscopy is a tool that can be used to rapidly and accurately analyze mammary gland structure. [DOI: 10.1117/1.2065827]

Keywords: reflectance confocal microscopy; mouse model; mammary gland; breast cancer; development.

Paper SS04228RR received Nov. 24, 2004; revised manuscript received May 4, 2005; accepted for publication May 6, 2005; published online Oct. 4, 2005.

1 Introduction

Breast cancer begins with aberrant growth in the mammary epithelial structure of the mammary gland. Over the past two decades a series of genetically engineered mouse models have been developed to improve our understanding of this process.[1] Traditionally, the mammary ductal structures of these mice are examined after excision from the animal. This is followed by either mounting of the fixed whole mammary gland on a glass slide after staining, or tissue sectioning after fixation/embedding with examination by conventional light microscopy.[2,3] This study explored the utility of reflectance cellular confocal imaging as a method to examine the ductal epithelial structure of the mammary gland *in situ* in the mouse without fixation and staining.

Address all correspondence to Priscilla A. Furth, Georgetown University, Lombardi Comprehensive Cancer Center, 3970 Reservoir Rd NW, Research Bldg. 520A, Washington, DC 20057. Tel.: (202) 687-8986; Fax: (202) 687-7505; E-mail: paf3@georgetown.edu

Reflectance confocal imaging is a technique that exploits different reflectance properties of subcellular structures to achieve virtual sectioning of intact tissue.[4] Contrast agents such as acetic acid, toluidine blue, and hypertonic saline can be used to selectively increase the brightness of nuclear structures (acetic acid and toluidine blue) or cytoplasm[5,6] (hypertonic saline). The technique has been used successfully to perform optical sectioning of normal and cancerous skin[4,7–9] and for detection of malignancy in the oral cavity,[10] liver,[11,12] and parathyroid glands.[13] Tissue phantoms have been used to demonstrate the feasibility of combining reflectance confocal imaging with targeted antibodies conjugated to gold nanoparticles.[14]

In this paper the effectiveness of the technique for evaluating normal and malignant mouse mammary gland structures in unfixed non-embedded tissue is examined. Both molecular medicine and developmental biology endeavor to correlate morphology with gene expression and activity. When tissue

1083-3668/2005/10(5)/051602/6/$22.00 © 2005 SPIE

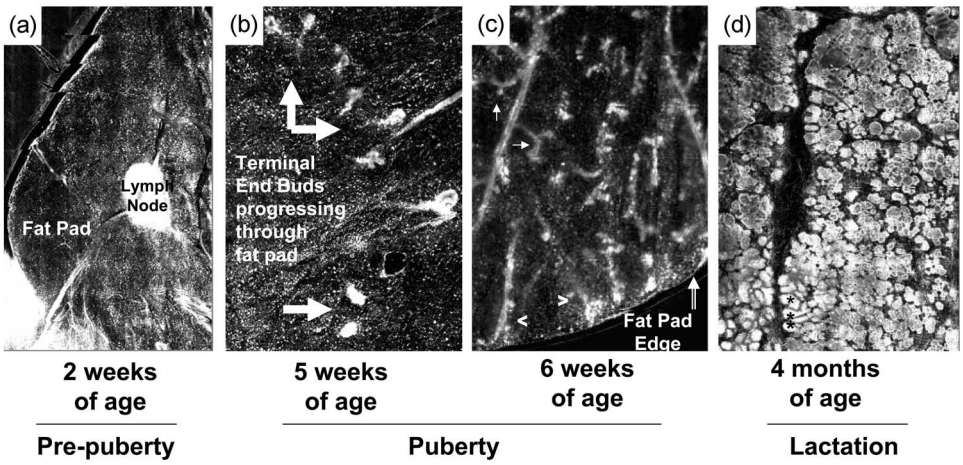

Fig. 1 Reflectance confocal microscopy of mammary gland development through puberty to lactation. (a) Imaging of the inguinal (fourth) mammary gland in a prepubertal female 2-week-old mouse. The central lymph node appears as a relatively highly reflecting structure in comparison to the surrounding fat pad. No mammary ducts were visualized. (b) Imaging of the inguinal mammary gland in a 5-week-old female mouse approximately 2 weeks after initiation of puberty. Relatively highly reflecting primary ducts with TEBs (indicated by wide white arrows) are seen coursing through the fat pad. (c) Imaging of the inguinal mammary gland in a 6-week-old female mouse approximately 3 weeks after initiation of puberty. The primary ducts (^) have reached the edge of the fat pad (double arrow) and secondary branching is evident (thin white arrows). (d) Imaging of the inguinal mammary gland in a 4-month-old female mouse during lactation. Grapelike clusters of alveolar development (*) filling the fat pad are evident. Contrast agent: 5% acetic acid.

can be accurately imaged without fixation and embedding, then this same tissue can be used for additional studies that aim to correlate biochemical and molecular events with specific structures. Normal wild-type mice and two different genetically modified mouse models were examined: conditional estrogen receptor α in mammary tissue (CERM) mice that exhibit abnormal ductal development with ductal carcinoma *in situ*[15] (DCIS) and mammary adenocarcinoma estrogen receptor α conditional (MAERC) mice, transgenic mice that develop invasive mammary carcinomas. Different physiological time points were examined in wild-type mice to create a series of digital images that represent prepuberty, puberty, and lactation and verify that reflectance confocal microscopy can be used to define normal developmental structures in the mammary gland. Genetically engineered mouse (GEM) models were studied to test whether reflectance confocal microcopy could be used to identify abnormal mammary gland ductal development and mammary adenocarcinomas in unfixed nonembedded mammary tissue.

Normal mammary gland development is characterized by a well-defined series of structural changes that are initiated during puberty and continue during pregnancy. Terminal end buds (TEBs) are the growing structures at the ends of mammary ducts that appear during puberty and are specifically susceptible to malignant transformation.[16,17] As puberty proceeds, secondary and tertiary branches appear off the primary ducts.[18] Vessels form around the developing ductal epithelial structures.[19] Mammary gland adenocarcinomas develop from ductal epithelium and invade into the surrounding mammary fat pad.[20] To validate the technique direct comparisons were made with carmine-alum whole-mount images and hematoxylin and eosin (H&E)-stained sections.

In summary, in the mouse mammary gland reflectance confocal imaging can be used to identify, optically section, and map terminal end buds; normal and abnormal ductal and alveolar structures; the network of vasculature structures that surround the ducts; and mammary adenocarcinomas.

2 Materials and Methods

2.1 *Mouse Models*

Mammary glands from wild-type C57B1/6 female mice were examined at different developmental and physiological time points: nonpregnant 2-, 5-, 6-, and 8-week-old-mice and lactating 4-month-old mice by reflectance confocal microscopy. Abnormal mammary gland development and adenocarcinomas were imaged in mammary glands from 4-month-old CERM C57B1/6 female mice[15] (MMTV-rtTA/tet-op-ERα, transgenic mouse model of ERα dependent abnormal mammary duct development) and 14-month-old MAERC C57B1/6 female mice[20] (MMTV-tTA/tet-op-ERα/tet-op-TAg, transgenic mouse model of ERα-driven mammary adenocarcinoma development). All animal procedures were approved by the Georgetown Animal Use and Care Committee.

2.2 *Reflectance Confocal Microscopy*

Reflectance confocal microscopy was performed using an instrument from VivaCell-TiBa (Rochester, New York, USA). A dilute (5%) acetic acid solution was used as a contrast agent to enhance visualization of the nuclei within cells by promoting condensation of nuclear material. RNALater (Qiagen, Valencia, California, USA) was used as a contrast agent for vascular structures by initiating blood coagulation. Prior to reflectance confocal imaging, mice were euthanized, followed by a midline incision to expose the mammary glands. For imaging, the entire mouse was placed on the reflectance confocal microscope with the lens underlying the mammary gland. Z-stack imaging (VivaStack) on the VivaCell-TiBa consists of 16 optical sections through the tissue at a user

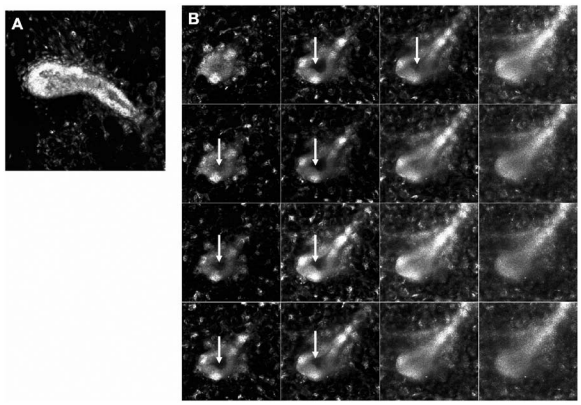

Fig. 2 Reflectance confocal microscopy of TEBs: (a) TEB from the inguinal mammary gland of a 5-week-old female mouse approximately 2 weeks after initiation of puberty. The characteristic globular appearance at the ductal end is well visualized. (b) Optical sectioning (Z-series) through a TEB from the mammary gland of a 5-week-old female mouse demonstrating the lumen (arrows), which forms behind the leading edge of the TEB. TEBs are the actively growing ends of mammary ducts that extend through the mammary fat pad during puberty in the mouse. Contrast agent: 5% acetic acid.

defined depth. Each image is 500×500 μm. In the studies presented here, Z-stack imaging was performed in 3.5-μm increments and viewed as sequential individual images. VivaBlock was used to map large areas of interest. VivaBlock is a composite of horizontally tiled images, each 500×500 μm. The size of the macroscopic map is user defined and can range from 2 to 20 mm^2. In the studies presented here, 6-mm^2 squares were used for mapping.

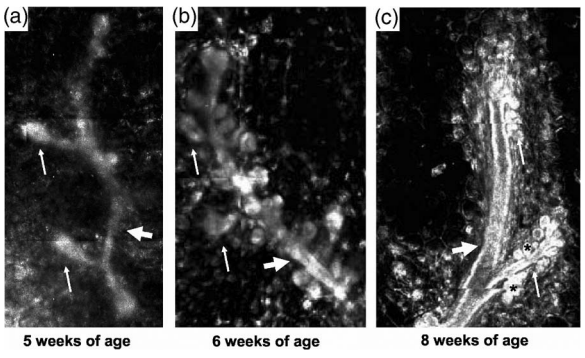

Fig. 3 Development of primary, secondary, and tertiary ductal branching in the mammary gland during puberty imaged by reflectance confocal microscopy. (a) Primary duct (wide white arrow) with some secondary ducts (thin white arrows) in the inguinal mammary gland of a 5-week-old female mouse approximately 2 weeks after initiation of puberty. (b) Primary duct (wide white arrow) with extensive secondary ductal branching (thin white arrows) in the inguinal mammary gland of a 6-week-old female mouse. (c) Primary duct (wide white arrow) with extensive secondary ductal branching (thin white arrows) and some tertiary branching (*) in the inguinal mammary gland of an 8-week-old female mouse. Contrast agent: 5% acetic acid.

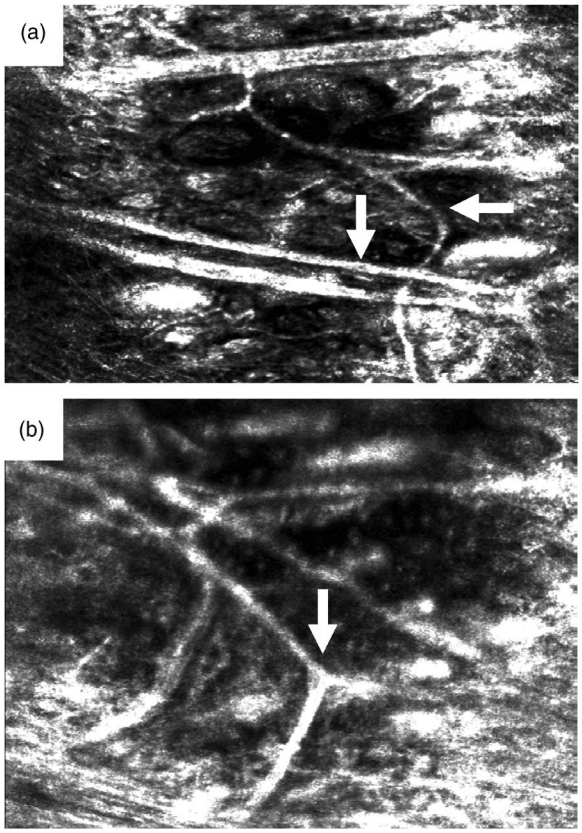

Fig. 4 Imaging of vasculature structure in the mammary gland using reflectance confocal microscopy. Two representative images of the vascular network in the inguinal mammary gland of a 2-week-old female mouse. Arrows point to typical vasculature structures. Contrast agent: RNALater.

2.3 *Imaging of Carmine-Alum Whole Mounts and H&E Stained Sections*

After reflectance confocal imaging, the mammary glands were removed, fixed, and stained with carmine-alum for whole-mount examination, or formalin-fixed, embedded, and 5-μm sections prepared for H&E staining, as described previously.[2] Whole mounts and H&E-stained sections were imaged on an Eclipse E800M microscope (Nikon Instruments Inc., Melville, New York, USA).

3 Results

3.1 *Imaging Ductal and Alveolar Mammary Gland Development*

Reflectance confocal microscopy was used to follow normal stages of mammary gland development from puberty through lactation (Fig. 1). At 2 weeks of age there is no more than minimal ductal development and only the fat pad and central lymph node were visualized [Fig. 1(a)]. By 5 weeks of age, TEBs, the growing ends of the ducts, were seen progressing through the fat pad [Fig. 1(b), wide white arrows]. By 6 weeks of age, the ducts reached the edge of the fat pad [Fig. 1(c), double lined arrow] and secondary branches have appeared (thin white arrows). Rounded grapelike alveolar devel-

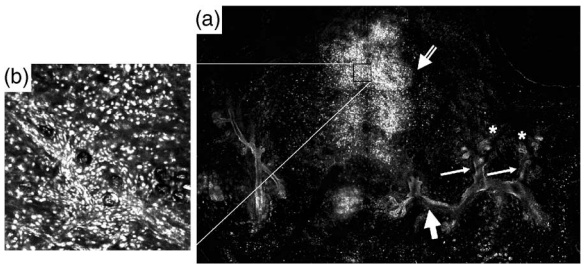

Fig. 5 Imaging of a mammary adenocarcinoma using reflectance confocal microscopy. (a) The nuclei of mammary adenocarcinoma cells in the mammary gland of a 14-month-old genetically engineered female MAERC mouse are more reflectant than the nuclei of the surrounding cells in the fat pad. Extension into the fat pad at the edges of the tumor can be seen (double lined arrow). Relatively normal appearing primary (wide white arrow), secondary (thin white arrows), and tertiary (*) ducts can be seen in the adjacent area. (b) Higher power image of the mammary adenocarcinoma tissue demonstrating the relatively dense organization of the highly reflecting nuclei of the malignant mammary epithelial cells. Contrast agent: 5% acetic acid.

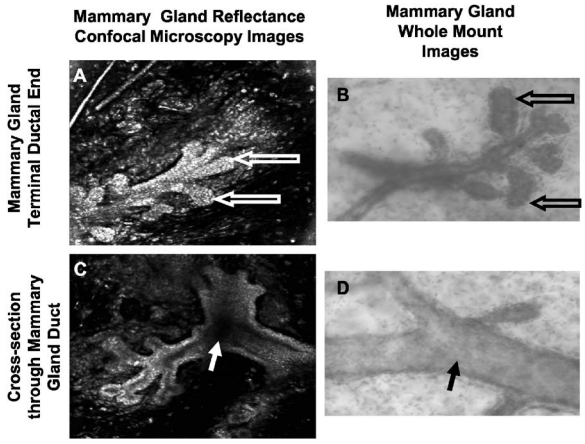

Fig. 6 Comparison of reflectance confocal microscopy with light microscopy of carmine-alum-stained mammary gland whole mounts. (a) Reflectance confocal microscopy image of the terminal end of a duct from the mammary gland of a 14-month-old genetically engineered female MAERC mouse (open arrows). Contrast agent: 5% acetic acid. (b) Light microscopy image of the terminal end of a duct from the mammary gland of the same 14-month-old genetically engineered female MAERC mouse (open arrows). (c) Reflectance confocal microscopy image of the cross section of a duct (closed arrow) from the mammary gland of a 14-month-old genetically engineered female MAERC mouse. Contrast agent: 5% acetic acid. (d) Light microscopy image of a the cross section of a duct (closed arrow) from the mammary gland of the same 14-month-old genetically engineered female MAERC mouse. Open arrows indicate equivalent structures in (a) and (b). Solid arrows indicate equivalent structures in (c) and (d).

opment at lactation [Fig. 1(d), *] was clearly distinguishable from the tubular development during puberty [Fig. 1(c), ^].

3.2 *Optical Sectioning of a TEB*

TEBs were identified on reflectance confocal microscopy by their characteristic globular appearance at ductal ends [Fig. 2(a)]. Z-stack imaging with optical sectioning through the internal structure of a TEB revealed internal lumen formation [Fig. 2(b), white arrows].

3.3 *Visualization of Primary, Secondary, and Tertiary Branching in the Mammary Gland*

At 5 weeks of age, relatively widely separated secondary branches point off a primary duct [Fig. 3(a), primary duct indicated by thick arrow, secondary ducts indicated by thin arrows]. At 6 weeks of age the number of secondary ducts was significantly increased [Fig. 3(b), primary duct indicated by thick arrow, representative secondary ducts indicated by thin arrows]. By 8 weeks of age, small tertiary ducts were found branching off an extended secondary duct [Fig. 3(c), primary duct, thick arrow; secondary ducts, thin arrows; tertiary ducts, *].

3.4 *Demonstration of Vasculature Structure in the Mammary Gland*

Vascular structures were not effectively imaged when acetic acid was used as the contrast agent. However, the use of RNALater as a contrast agent selectively enhanced visualization of the vascular network (Fig. 4, arrows indicate representative vessels). After imaging, the tissue was kept in RNALater overnight at 4°C and removed and frozen at −70°C the next morning, and high-quality RNA was extracted several weeks later (data not shown).

3.5 *Mapping Adenocarcinomas and Ducts within the Mammary Fat Pad*

The mapping function of the reflectance confocal microscope was used to localize an adenocarcinoma (double arrow) and surrounding ductal structures in the fat pad of a genetically engineered MAERC mouse [Fig. 5(a)]. The adenocarcinoma appeared as a dense collection of reflective cell nuclei [Fig. 5(b)]. Normal-appearing mammary gland ductal structures with primary (thick arrow), secondary (thin arrow) and tertiary branches (*) were found adjacent to the adenocarcinoma.

3.6 *Comparison of Reflectance Confocal Microscopy with Light Microscopy of Carmine-Alum Stained Mammary Gland Whole Mounts*

Equivalent images were taken with reflectance confocal microscopy of unfixed nonmounted mammary glands *in situ* and with conventional light microscopy of carmine-alum stained whole mounts (Fig. 6). Comparable images of secondary branches at the terminus of mammary gland ducts [Figs. 6(a) and 6(b), open arrows] and cross sections of ducts [Figs. 6(c) and 6(d), solid arrows] were found on reflectance confocal microscopy and conventional microscopy of a carmine-alum-stained whole mount. Reflectance confocal imaging was more time-efficient than conventional microscopy of carmine-alum-stained whole mounts because imaging was performed immediately on unfixed and unmounted *in situ* specimens at the time of necropsy. In contrast, carmine-alum-stained whole mounts imaging by light microscopy was performed only days after the mammary glands were removed from the mouse and required hours of preparation time.

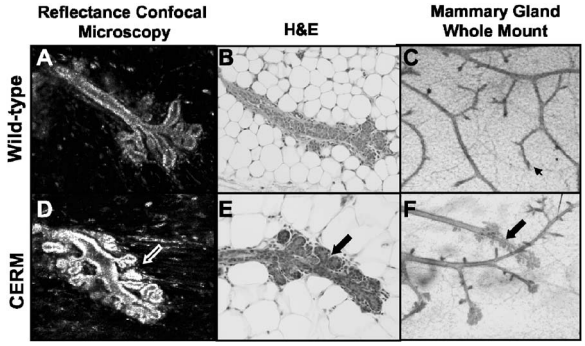

Fig. 7 Comparison of reflectance confocal microscopy with light microscopy of H&E-stained sections of mammary gland tissue. (a) Reflectance confocal microscopy image of the normal terminal end of a duct from the mammary gland of a 4-month-old female wild-type mouse. Contrast agent: 5% acetic acid. (b) Light microscopy image of and H&E-stained section of mammary tissue from a 4-month-old female wild-type mouse demonstrating normal terminal ductal end structure. (c) Light microscopy image of a carmine-alum-stained whole mount of a mammary gland from a wild-type 4-month-old female mouse demonstrating normal terminal ductal ends (small black arrow). (d) Reflectance confocal microscopy image of the terminal ductal end from the mammary gland of a 4-month-old genetically engineered female CERM mouse demonstrating lateral budding (large white arrow). Contrast agent: 5% acetic acid. (e) Light microscopy image of an H&E-stained section of mammary tissue from the mammary gland of a 4-month-old genetically engineered female CERM mouse demonstrating lateral budding (large black arrow). (f) Light microscopy image of a carmine-alum-stained whole mount of a mammary gland from a 4-month-old genetically engineered female CERM mouse demonstrating lateral budding (large black arrow).

3.7 *Comparison of Reflectance Confocal Imaging with Light Microscopy of H&E Stained Sections*

Analogous images of ductal structures were found using reflectance confocal imaging and conventional light microscopy of H&E stained sections (Fig. 7). Ductal end structures were compared in mature 4-month-old wild-type and genetically engineered CERM mice. One of the characteristic pathological findings in the 4-month-old CERM mice was the abnormal lateral budding that extended along the duct away from the terminal end [Figs. 7(d)–7(f) arrows]. In CERM mice, abnormal persistent estrogen-mediated growth signals result in numerous abortive branches termed lateral budding.[15] Normal development of ductal branching during puberty is also initiated by budding (Fig. 3) but resolves into a normal branching pattern by 4 months of age [Figs. 7(a)–7(c)].

4 Discussion and Summary

Reflectance confocal microscopy can be used to analyze changes in mammary gland morphology through both normal development and cancer progression. TEBs were specifically identified as well as the extent of ductal penetration through the fat pad during puberty. The milk-producing alveolar structures that develop at the end of pregnancy were clearly distinguishable from the purely ductal structures found in the nonpregnant gland. Development of mammary cancers from the ducts were visually identifiable. Imaging quality of unfixed, nonembedded tissue *in situ* performed at the time of necropsy using reflectance confocal microscopy was comparable to that achieved by light microscopy after tissue fixation and embedding. The most immediate advantage of reflectance confocal microscopy was that it can be performed on nonfixed, nonembedded *in situ* specimens promptly at the time of necropsy. Other benefits were the rapid acquisition of images for analysis coincident with necropsy, the ability to use the imaged and morphologically characterized tissue in follow-up experiments, and the capacity to readily sample and optically section an unrestricted number of areas within the tissue. This last attribute enables an investigator to rapidly and economically survey an entire tissue without laborious processing and serial sectioning of fixed embedded specimens, which may preclude use of the same tissue for other types of experiments. Serial Z-stack images can be used for 3-D reconstructions of TEBs and cancers, enabling an investigator to follow the invasion of these structures into surrounding tissue. Acquisition of real-time images of pathology at the time of necropsy enables an investigator to immediately initiate follow-up diagnostic and mechanistic studies, rather than having to wait for the more laborious conventional processing and staining of tissue samples. Confocal reflectance imaging will clearly be a useful tool in future studies for the analysis of mammary gland structure and mammary cancer development.

Acknowledgments

These studies were supported in part by Department of Defense (DAMD 17-01-1-0310 to P.A.F.), a Training Grant in Tumor Biology from the National Cancer Institute (NCI), National Institutes of Health (NIH) (2T32CA09686-08 for M.T.T.), and the Susan G. Komen Breast Cancer Foundation (PDF0402444 to P.A.F.).

References

1. R. D. Cardiff, D. Moghanaki, and R. A. Jensen, "Genetically engineered mouse models of mammary intraepithelial neoplasia," *J. Mam. Gland. Biol. Neoplas.* **5**, 421–437 (2000).
2. M. Li, J. Hu, K. Heermeier, L. Hennighausen, and P. A. Furth, "Apoptosis and remodeling of mammary gland tissue during involution proceeds through P53-independent pathways," *Cell Growth Differ.* **7**, 13–20 (1996).
3. J. M. Strum, "A mammary gland whole mount technique that preserves cell fine structure for electron microscopy," *J. Histochem. Cytochem.* **27**, 1271–1274 (1979).
4. S. Gonzalez, K. Swindells, M. Rajadhyaksha, and A. Torres, "Changing paradigms in dermatology: confocal microscopy in clinical and surgical dermatology," *Clin. Dermatol.* **21**, 359–369 (2003).
5. R. A. Drezek, T. Collier, C. K. Brookner, A. Malpica, R. Lotan, R. R. Richards-Kortum, and M. Follen, "Laser scanning confocal microscopy of cervical tissue before and after application of acetic acid," *Am. J. Obstet. Gynecol.* **182**, 1135–1139 (2000).
6. A. F. Zuluaga, R. Drezek, T. Collier, R. Lotan, M. Follen, and R. Richards-Kortum, "Contrast agents for confocal microscopy: how simple chemicals affect confocal images of normal and cancer cells in suspension," *J. Biomed. Opt.* **7**, 398–403 (2002).
7. C. Curiel-Lewandrowski, C. M. Williams, K. J. Swindells, S. R. Tahan, S. Astner, R. A. Frankenthaler, and S. Gonzalez, "Use of in vivo confocal microscopy in malignant melanoma: an aid in diagnosis and assessment of surgical and nonsurgical therapeutic approaches," *Arch. Dermatol.* **140**, 1127–1132 (2004).
8. S. P. Hicks, K. J. Swindells, M. A. Middelkamp-Hup, M. A. Sifakis, E. Gonzalez, and S. Gonzalez, "Confocal histopathology of irritant contact dermatitis in vivo and the impact of skin color (black vs white)," *J. Am. Acad. Dermatol.* **48**, 727–734 (2003).
9. K. Swindells, N. Burnett, F. Rius-Diaz, E. Gonzalez, M. C. Mihm, and S. Gonzalez, "Reflectance confocal microscopy may differentiate acute allergic and irritant contact dermatitis in vivo," *J. Am. Acad.*

Dermatol. **50**, 220–228 (2004).
10. A. L. Clark, A. M. Gillenwater, T. G. Collier, R. Alizadeh-Naderi, A. K. El Naggar, and R. R. Richards-Kortum, "Confocal microscopy for real-time detection of oral cavity neoplasia," *Clin. Cancer Res.* **9**, 4714–4721 (2003).
11. V. Campo-Ruiz, E. R. Ochoa, G. Y. Lauwers, and S. Gonzalez, "Evaluation of hepatic histology by near-infrared confocal microscopy: a pilot study," *Hum. Pathol.* **33**, 975–982 (2002).
12. V. Campo-Ruiz, G. Y. Lauwers, R. R. Anderson, E. Delgado-Baeza, and S. Gonzalez, "*In vivo* and *ex vivo* virtual biopsy of the liver with near-infrared, reflectance confocal microscopy," *Mod. Pathol.* **18**, 290–300 (2004).
13. W. M. White, G. J. Tearney, B. Z. Pilch, R. L. Fabian, R. R. Anderson, and R. D. Gaz, "A novel, noninvasive imaging technique for intraoperative assessment of parathyroid glands: confocal reflectance microscopy," *Surgery (St. Louis)* **128**, 1088–1100 (2000).
14. K. Sokolov, M. Follen, J. Aaron, I. Pavlova, A. Malpica, R. Lotan, and R. Richards-Kortum, "Real-time vital optical imaging of precancer using anti-epidermal growth factor receptor antibodies conjugated to gold nanoparticles," *Cancer Res.* **63**, 1999–2004 (2003).
15. M. S. Frech, E. D. Halama, M. T. Tilli, B. Singh, E. J. Gunther, L. A. Chodosh, J. A. Flaws, and P. A. Furth, "Deregulated estrogen receptor alpha expression in mammary epithelial cells of transgenic mice results in the development of ductal carcinoma *in situ*," *Cancer Res.* **65**, 681–685 (2005).
16. N. J. Kenney, G. H. Smith, E. Lawrence, J. C. Barrett, and D. S. Salomon, "Identification of stem cell units in the terminal end bud and duct of the mouse mammary gland," *J. Biomed. Biotechnol.* **1**, 133–143 (2001).
17. J. Russo and I. H. Russo, "Experimentally induced mammary tumors in rats," *Breast Cancer Res. Treat.* **39**, 7–20 (1996).
18. A. Lochter, "Plasticity of mammary epithelia during normal development and neoplastic progression," *Biochem. Cell Biol.* **76**, 997–1008 (1998).
19. V. Djonov, A. C. Andres, and A. Ziemiecki, "Vascular remodelling during the normal and malignant life cycle of the mammary gland," *Microsc. Res. Tech.* **52**, 182–189 (2001).
20. M. T. Tilli, M. S. Frech, M. E. Steed, K. S. Hruska, M. D. Johnson, J. A. Flaws, and P. A. Furth, "Introduction of estrogen receptor-alpha into the TTA/TAg conditional mouse model precipitates the development of estrogen-responsive mammary adenocarcinoma," *Am. J. Pathol.* **163**, 1713–1719 (2003).